Biosensors and Bioelectronics 25 (2010) 2483–2489

Contents lists available at ScienceDirect

Biosensors and Bioelectronics

journal homepage: www.elsevier.com/locate/bios

Electrochemical DNA biosensor based on proximity-dependent DNA ligation assays with DNAzyme amplification of hairpin substrate signal

Chenhu Sun, Liangliang Zhang, Jianhui Jiang, Guoli Shen, Ruqin Yu*

State Key Laboratory of Chemo/Biosensing and Chemometrics, College of Chemistry and Chemical Engineering, Hunan University, Changsha 410082, PR China

ARTICLE INFO

Article history:
Received 6 February 2010
Received in revised form 9 April 2010
Accepted 9 April 2010
Available online 24 April 2010

Keywords:
DNAzyme
Electrochemical DNA biosensor
Proximity ligation

ABSTRACT

This paper describes a novel electrochemical DNA sensor for the simple, sensitive and specific detection of nucleic acids based on proximity-dependent DNA ligation assays with the DNAzyme amplification of hairpin substrate signal. A long DNA strand contains the catalytic motif of Mg^{2+}-dependent 10-23 DNAzyme, acting as the recognition probe. When the target DNA was introduced into the system, part of it was complementary to 5′-end of the recognition probe, resulting in the ligation of a stable duplex, the unbinded part of the target DNA was acted as one binding arm for the DNAzyme. This duplex containing a complete 10-23 DNAzyme structure could cleave the purine–pyrimidine cleavage site of the hairpin substrate, which resulted in the fragmentation of the hairpin structure and the release of two single-stranded nucleic acids, one of which was biotinylated and acted as the signal probe. An immobilized thiolated capture probe could bind with the signal probe, using biotin as a tracer in the signal probe, and streptavidin–alkaline phosphatase (SA–ALP) as reporter molecule. The activity of the immobilized enzyme was voltammetrically determined by measuring the amount of 1-naphthol generated after 5 min of enzymatic dephosphorylation of 1-naphthyl phosphate. The results revealed that the sensor showed a sensitive response to complementary target sequences of *H. pylori* in a concentration range from 100 fM to 1 nM, with a detection limit of 50 fM. In addition, the sensing system could discriminate the complementary sequence from mismatched sequences, with high sensitivity and reusability.

1. Introduction

Catalytic nucleic acids derived by in vitro selection (Osborn and Ellington, 1997; Tuerk and Gold, 1990) represent a new class of detection tools that possess unique features (Breaker, 1999, 2000). These artificially designed nucleic acid sequences (ribozymes, deoxyribozymes and aptazymes) can fold into well-ordered, three-dimensional structures that catalyze specific chemical reactions (Lu and Liu, 2006). Among the many studies demonstrating the potential of catalytic nucleic acids, those involving deoxyribozymes or DNAzymes, have attracted much attention.

DNAzymes are generally composed of two functional domains: the catalytic loop that recognizes specific ion employed as coenzyme and the binding arm that targets its complementary sequence or substrate. Indeed, numerous recent studies used DNAzymes to analyze various metal ions (Xiao et al., 2007a,b; Yin et al., 2009; Lee et al., 2008). Also, different DNAzyme probes were used to develop different amplified bioanalytical assays for nucleic acid detection (Elbaz et al., 2009; Sando et al., 2003, 2005; Tian and Mao, 2005). DNAzymes could achieve its target specificity by Watson–Crick interactions which occur via two substrate-binding domains, discriminating between a series of closely related substrate sequences (Cairns et al., 2000).

Nowadays, sensitive and selective DNA detection has become increasingly important in diagnosis, gene therapy and other biomedical studies. Tools for accurate, sequence-specific DNA analysis are essential for the efficient use of genomic information. Motivated by the desire for rapid, simple means of DNA analysis, recent years have seen the development of fluorescent and colorimetric DNAzyme sensors for DNA detection. A DNAzyme cascade by the cooperative self-assembly of multicomponent nucleic acid structures was developed for the analysis of DNA with a detection limit that corresponded to 1 pM (Elbaz et al., 2009). A first-generation fluorescence-reporting target-assisted self-cleavage (TASC) probe which acts as a multiple-turnover substrate was reported for the target DNA as a catalyst (Sando et al., 2003). A second-generation TASC probe to the nucleic acid sensing based on the switching-on of incorporating DNAzyme activity upon the target-induced conformational change was then reported by the same research group (Sando et al., 2005). Catalytic molecular beacons were constructed from a hammerhead-type DNAzyme which can detect DNA down to a concentration of 8 nM (Stojanovic

* Corresponding author. Tel.: +86 731 88822577; fax: +86 731 88822577.
E-mail address: rqyu@hnu.cn (R. Yu).

0956-5663/$ – see front matter © 2010 Elsevier B.V. All rights reserved.
doi:10.1016/j.bios.2010.04.012

et al., 2001). An improved catalytic molecular beacon was reported with a detection of 10 pM DNA (Tian and Mao, 2005).

However, some of these optical methods may have possible disadvantages including poor detection limit due to the large background (Elbaz et al., 2009). Recently significant efforts have been devoted to improve the sensitivity and accuracy of DNA detection (Zhang et al., 2009a,b; Gong et al., 2009; Xiao et al., 2009). Electrochemical methods benefit from the miniaturization of modern microelectronics and exhibit relatively low background. Thus, electrochemical sensors are less likely to suffer from these potential drawbacks. Compared to optical DNAzyme sensors, however, the development of electrochemical DNAzyme sensors is still in its rudimentary stage.

In the present work, a simple, signal-on electrochemical DNAzyme sensor for DNA detection is reported for the first time. According to the literature, the proximity ligation assay (Fredriksson et al., 2002) depends on the simultaneous recognition of a target molecule by a pair of affinity probes. This brings the tail sequences of the affinity probe pair in proximity to hybridize together with a connector oligonucleotide followed by a ligation-based amplification and detection. The proximity-dependent surface hybridization assays have been reported for proteins (Zhang et al., 2007) and DNA detection (Zhang et al., 2009a,b) in this laboratory. Here we propose a novel strategy based on the principle of proximity-dependent DNA ligation assays for DNA detection. The coordinated and proximal binding of the target DNA by the recognition probe promotes ligation of the two oligonucleotides, using part of the target sequence as one binding arms of the DNAzyme and thus giving rise to a complete structure of the DNAzyme whose catalytic ability could reflect the amount of the target DNA. The activation of DNAzyme could amplify the recognition events by multiple cleavages of biotinylated hairpin substrate. The biotin–streptavidin interaction as a well-established amplification system (Zhang et al., 2009a,b; Miranda-Castro et al., 2007; Lucarelli et al., 2006; Munge et al., 2005) was used for amplifying the signal after hybridization between the capture probe and signal probe. Compared with other electrochemical DNA sensors, our new system has two main advantages. First, we use the 10-23 DNAzyme and the streptavidin–alkaline phosphatase (SA–ALP) as coupled biocatalysts for the signal amplification. On the one hand, when the DNAzyme is hybridized with its substrate sequence and the desired cation binds to the catalytic loop, hydrolysis of the substrate sequence is activated. Because of the lower affinity of the cleaved hairpin substrate, the DNAzyme can bind to yet another substrate so that it can be recycled for the hydrolysis of multiple substrates in a manner similar to that of enzymes with their substrate target. On the other hand, the incorporation of an enzyme (alkaline phosphatase) for generating the output electrochemical signal offers the potential for signal amplification, further improving the sensitivity. Second, we take advantages of both the homogeneous reaction and the electrochemical detection. The homogeneous system avoids the complex and time-consuming procedures, thereby achieving a rapid and simple reaction process. Moreover, the combination of an electrochemical platform has allowed the simplification of the detection and increased the sensitivity of the measurements. Compared with some ultrasensitive electrochemical DNA sensors with lower detection limit (Azek et al., 2000; Takenaka et al., 2000), which could only discriminate between complementary and non-complementary DNA sequences, our method could successfully discriminate the target DNA from various DNA sequences with one or more mismatches, proving to be practically useful for sensitive single-nucleotide polymorphism detection and point mutation identification. In addition, while above-mentioned methods may depend on complex handling procedures such as PCR amplification and time-consuming synthetic ligand, our method holds great promise for low-cost, low volume and rapid readout of a target DNA sequence.

2. Experimental

2.1. Chemicals and reagents

The DNA oligonucleotides were synthesized by Takara Biotechnology Co. Ltd. (Dalian, China). Streptavidin–alkaline phosphatase (SA–ALP), diethypyrocarbonate (DEPC) and bovine serum albumin (BSA) were supplied by Dingguo Bio-technology Co. Ltd. (Beijing, China). 1-Naphthyl phosphate disodium salt was obtained from Sigma–Aldrich Chemical Co. Magnesium chloride hexahydrate was purchased from Shanghai Sangon Biological Engineering Technology & Services Co., Ltd. (Shanghai, China). N,N-dimethylformamide (DMF, 99.5%) was purchased from Tianjin Damao Chemical Reagent Factory (Tianjin, China). All of the other chemicals were of analytical reagent grade and used without further purification. DEPC was used in the experiments to inactivate the RNases from water and other laboratory utensils. DEPC treated DNase/RNase free ultrapure water was used for all buffers and stock solutions of oligonucleotides throughout this work.

2.2. Apparatus

The biosensors were measured via differential pulse voltammetry (DPV) and electrochemical impedance spectroscopy (ESI) with a CHI 760B electrochemical workstation (Shanghai Chenhua Equipments, China). The three-electrode system consisted of gold electrode (2 mm diameter) as the working electrode, a KCl saturated calomel electrode (SCE) as the reference electrode and a platinum wire as the counter electrode. All electrochemical measurements were performed in 0.5 M Tris–HCl (pH 9.6) containing 10 mM Mg^{2+} at room temperature.

Table 1
Oligonucleotide sequences used in the experiments[a].

Note	Sequence (5′ → 3′)
Recognition probe	TTCCAAAGGGCAGTCA**GGCTAGCTACAACGA**CCTATGTGA
Hairpin substrate	CCGTCACATAGG*ra*UGAGATCATTGACGG-biotin
Capture probe	CCGTCAATGATCTC-$(CH_2)_6$-SH
Target DNA	TCAATGATCCTGCCCTTTGGAACGC
Single-base mismatched 1	TCAATGATCCTGCCCTATGGAACGC
Single-base mismatched 2	TCAATGATCCTGCCGTTTGGAACGC
Single-base mismatched 3	TCAATGATCCTGGCCTTTGGAACGC
Single-base mismatched 4	TCAATCATCCTGCCCTTTGGAACGC
Single-base mismatched 5	TCTATGATCCTGCCCTTTGGAACGC
Four-base mismatched	TCATTGAACCTGGCCTATGGAACGC
Non-complementary	TCTGATACGTACCTCTAGTGCAGTG

[a] 15-base catalytic motif (bold) of 10-23 DNAzyme, *ra* represents an adenine ribonucleotide, the mismatch positions (underlined).

2.3. Target and probes

The oligonucleotide sequences used in this work are listed in Table 1. As a target model, a 25-mer complementary target sequence of the pathogen bacterium *H. pylori* was selected. A recognition probe containing 15-base catalytic motif (bold) of the 10-23 DNAzyme sequence was used for ligation and catalysis events. The hairpin substrate contains an adenine ribonucleotide (ra) and a uridine ribonucleotide (U) in the loop sequence. The capture probe was a short thiolated DNA strand which was complementary to the signal probe generated from the hairpin substrate after the DNAzyme cleavage.

2.4. Immobilization of capture probe on gold electrode

The gold electrode was polished sequentially with 0.3 and 0.05 μM alumina powder, followed by ultrasonic cleaning in ethanol and ultrapure water. Then the gold electrode was cleaned with piranha solution, rinsed with ultrapure water, and electrochemically treated by cycling the potential between −0.3 and 1.5 V in 0.5 M H_2SO_4 at a scan rate of 0.1 V/s for 10 min. Finally, the electrode was washed with ultrapure water and dried under a nitrogen stream, and 10 μL of 1 μM thiolated capture probe solution was dropped onto the surface of the pretreated gold electrode and kept for 12 h at room temperature.

2.5. DNA hybridization

Different concentrations of the target DNA and recognition probe (10 nM) were incubated in 50 mM Tris–HCl buffer (pH 7.5) containing 10 mM $MgCl_2$ at 37 °C for 1 h. Cleavage reactions were initiated by the addition of the biotinylated hairpin substrate (100 nM, 10-fold molar excess) to the aforementioned solution to make a final volume of 100 μL and the incubation of the system at 37 °C for 1 h. Then the thiolated oligonucleotide functionalized electrode was immersed into the above-mentioned hybridization solution at 37 °C for 1 h to capture the signal probe.

2.6. Labeling with streptavidin–alkaline phosphatase

The electrode surface was rinsed in 10 mM PBS (pH 7.4, 10 mM Mg^{2+}) for 10 min. A 10 μL SA–ALP solution (1:100 dilution from the stock solution using 10 mM PBS containing 1% BSA) was applied to the electrode surface and incubated at 37 °C for 30 min.

2.7. Electrochemical detection

After the electrode was thoroughly rinsed twice by 10 mM PBS (pH 7.4, 10 mM Mg^{2+}) for 10 min, the electrode was incubated with 3 mL of 1-naphthyl phosphate solution (0.004 M in 0.5 M Tris–HCl, pH 9.6, containing 10 mM $MgCl_2$). After 5 min, the electrochemical signal of the enzymatically produced 1-naphthol was measured by DPV (modulation time, 0.05 s; interval time, 0.15 s; step potential, 5 mV; modulation amplitude, 70 mV; scan rate, 10 mV/s; pulse amplitude, 20 mV; potential scan, from 0 to 600 mV). Upon scanning the potential, the 1-naphthol exhibits an irreversible oxidation peak around 300 mV. This peak came from an electron transfer reaction of 1-naphthol and the height of it was taken as the analytical signal. All the results shown in this paper are the mean of three measures and the error bars correspond to the standard deviation.

3. Results and discussion

3.1. Principle of electrochemical DNA biosensor

Scheme 1 depicts the designed elements of the biosensor based on proximity-dependent DNA ligation assay. The recognition probe

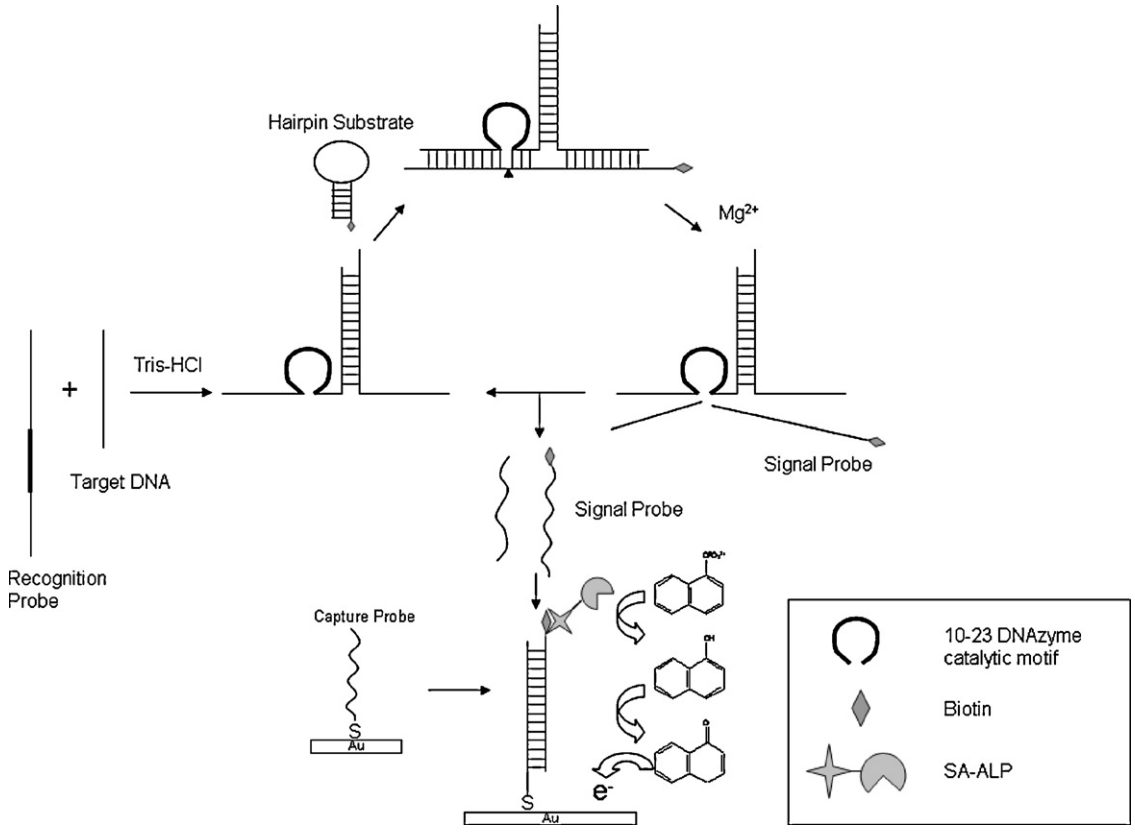

Scheme 1. Schematic drawing of the setup for the recognition and electrochemical detection of the target DNA sequence.

and the hairpin substrate were designed based on the melting temperatures in the system according to the target DNA sequence. The 5′-end of the recognition probe which includes a domain of the 10-23 DNAzyme was complementary to part of the target DNA. The recognition probe and the target DNA include respectively at their 3′ and 5′ ends the base sequences that are complementary to corresponding predesigned regions of the hairpin substrate, which were acted as two binding arms to open the hairpin structure. In the presence of the target DNA, the hairpin substrate could be opened and all of these components self-assembled into a duplex complex. Note that the components were predesigned in such a way that the self-assembled complex was generated only in the presence of the target DNA. The melting temperatures (calculated as ~45 °C using the Zuker program (Markham and Zuker, 2005)) for the recognition probe and the target DNA were designed to be higher than the reaction temperature (37 °C), while the melting temperatures for the hairpin substrate and the target DNA (~20 °C) as well as the hairpin substrate and the recognition probe (~24 °C) were both lower than the reaction temperature. Thus, the target DNA or the recognition probe alone could not yield stable structures with the hairpin substrate at a temperature of 37 °C used throughout the experiments. However, the ligation of 3′-end of the target DNA and 5′-end of the recognition probe drawn the residual parts of these two strands in proximity, which promoted cooperative hybridization of the residual complementary sequences of the target DNA and the recognition probe with the substrate. Thus, the complete DNAzyme structure was formed, using part of the target DNA sequence as one binding arm, part of the recognition probe as another binding arm, and the opened hairpin structure as the substrate. In the presence of Mg^{2+}, the hydrolytic cleavage between the paired pyrimidine base and the free purine base took place. This cleavage resulted in two single-stranded nucleic acids, one of which was biotinylated and acted as the signal probe. Because of the lower affinity of the cleaved hairpin substrate, the DNAzyme could bind to yet another substrate so that it could be recycled for the hydrolysis of multiple substrates in a manner similar to that of enzymes with their substrate target. The multiple cleavages gave rise to significantly increased amount of signal probes and thus realized the signal amplification.

In a buffer solution, the hairpin substrate adopted a stem–loop structure. Considering that the capture probe might bind with the excessive hairpin substrate to generate background signal, the melting temperature for the one-half of loop sequence of the hairpin substrate and the capture probe was designed to be lower than the reaction temperature, while the melting temperature for the cleaved signal probe and the capture probe was designed to be higher than the reaction temperature. When the modified electrode was immersed into the solution, the capture probe could not stably hybridize with one-half of the loop sequence of the hairpin substrate at a temperature of 37 °C, but instead would capture the cleaved signal probe to form a more stable duplex. Therefore, it was assumed that the long stem of the hairpin structure could prevent the capture probe from binding with the substrate and considerable background would not be generated. To confirm this assumption, we investigated the optimized capturing time for the thiolated capture probe to bind with the signal probe in the following discussion.

Transduction of the interfacial biorecognition events was accomplished by means of electrochemical measurements, using a streptavidin-conjugated enzyme label (alkaline phosphatase) that converted its electro-inactive substrate 1-naphthyl phosphate into an electroactive derivative 1-naphthol (Lucarelli et al., 2006; Del Giallo et al., 2005; Carpini et al., 2004). 1-Naphthol exhibited an irreversible oxidation peak around 300 mV in Tris–HCl. Additionally, 1-naphthyl phosphate was not electrochemically active in the potential window used (0–0.6 V). Thus, 1-naphthyl phosphate was selected as substrate of ALP to measure the activity of the immobilized enzyme. From the differential pulse voltammograms (Fig. 2), the biosensor showed obvious oxidation peak recorded in 0.5 M Tris–HCl (pH 9.6) containing 10 mM Mg^{2+}. The oxidation peak with 1 nM target DNA was more than 6.0 μA, about 15 times more than the blank background. The background signal might be attributed to the hydrolysis of the ribonucleo sites of the hairpin substrate. The apparent signal enhancement of current demonstrated this sensor was capable of target DNA detection.

3.2. Immobilization interface

Electrochemical impedance spectroscopy (EIS) was carried out to study the gold electrode modified by different procedures. As show in Fig. S1 (supplementary material), the impedance plot for the bare gold electrode (Fig. S1, curve a) exhibits an almost straight line, as characteristics of an electrochemical diffusional limiting process. Faraday impedance (Fig. S1, curve b) increased significantly because of the thiolated DNA capture probe modification. Electron transfer became more difficult because of the capture probe modification resulting in negative charge enhancement on the gold electrode surface. When the capture probe hybridized with the biotinylated signal probe, the hybridization process afforded further inhibition of ferricyanide from reaching the electrode surface, leading to further enhancement of the impedance (Fig. S1, curve c). This result demonstrated that the biotinylated signal probe which produced by DNAzymes cleavage could be captured by the thiolated capture probe.

3.3. Effect of SA–ALP dilution ratio and Mg^{2+} concentration

Experiments indicated that the SA–ALP dilution ratio obviously influences the signal (Fig. 1A, solid line) and the blank (Fig. 1A, dotted line) responses of the biosensor. The signal responses increased rapidly with the dilution ratio of SA–ALP up to 1:100, and the signal exhibited no further remarkable increase for SA–ALP with a lower dilution ratio. It could also be observed that the blank responses increased with the increasing dilution ratio. It is evident that the dilution ratio of 1:100 is a saturated concentration for the enzyme reaction. To obtain higher signal and lower background, the dilution ratio of 1:100 was selected throughout the experiments.

Mg^{2+} acts as a cofactor of the DNAzymes, the cleavage rate grows faster when the concentration of Mg^{2+} increases (Brown et al., 2003). Besides, the hybridization efficiencies were influenced by the Mg^{2+} ion concentration and a high Mg^{2+} concentration is disadvantageous for the dissociation of the two fragmented oligos after DNAzyme cleavage. So the effects of Mg^{2+} concentration on the signal responses were investigated. Fig. 1B shows the effects of Mg^{2+} concentration from 0 to 20 mM on the signal responses of the biosensor. One can observe that the highest signal value was obtained when the concentration of Mg^{2+} ions was 10 mM and that the signal decreased with increasing concentrations of Mg^{2+} ions (from 10 to 20 mM). This effect might be due to the higher concentration of Mg^{2+} influencing the dissociation of the signal probe. Therefore, 10 mM Mg^{2+} ions in buffer were used as the optimal concentration of Mg^{2+} ions in this work.

3.4. Optimization of the incubation time and the capturing time

The incubation time of the cleavage reaction also influence the performance of the sensor. Among all RNA-cleaving DNAzyme, the 10-23 DNAzyme is one of the most efficient enzymes (Joyce, 2004). In order to optimize the incubation time, the cleavage reaction was allowed to proceed for different periods of time followed by the hybridization of the recognition probe and the target DNA for 1 h. As shown in Fig. 1C, the peak current increased gradually with the augment of incubation time and then tended to be constant after about 45 min, which indicated that the equilibrium was

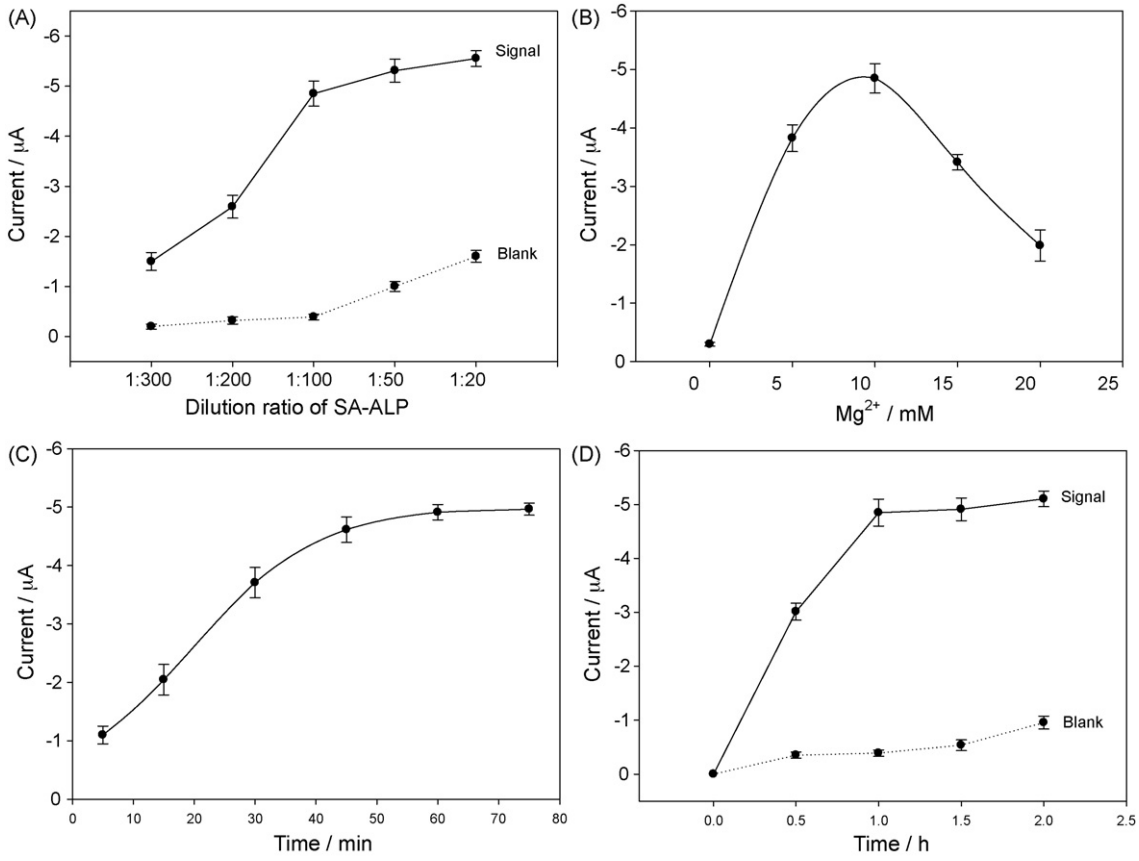

Fig. 1. Optimization of experimental conditions. (A) Effect of SA–ALP dilution ratio on peak current. The blank response is shown as the dotted line, and the signal response is shown as the solid line in the presence of 0.1 nM target DNA. The dilution solution of SA–ALP was 10 mM PBS (pH 7.4) containing 1% BSA. (B) Effect of Mg^{2+} concentration in Tris–HCl on peak current. The concentration of target DNA was 0.1 nM. (C) Plot of the peak current response versus the incubation time. The concentration of target DNA was 0.1 nM. (D) Optimization of the capturing time (from 0 to 2 h) in the presence of 0.1 nM target DNA (solid line) and blank (dotted line).

reached. To obtain the maximum hybridization efficiencies and cleavage of the substrate, 1 h was selected for the cleavage reaction.

Although the design of hairpin substrate could effectively prevent the capture probe from binding with the non-cleaved substrate, the capture probe might destabilize the stem of the hairpin substrate and then bind with one-half of the substrate sequence to generate background signal. Therefore, the capturing time was investigated. Fig. 1D shows the effect of capturing time on the signal response of the biosensor by immersing the thiolated oligonucleotide functionalized electrode into the hybridization solution containing 0.1 nM target DNA and the solution containing no target DNA for 2 h. The ratio of the signal to the blank background increased significantly as the capturing time increased up to 1 h, indicating improved hybridization performance. After 1 h, a slight signal enhancement could be observed. However, the background continued to increase with the capturing time, which might be attributed to the minor disturbance of the capture probe to the structure of the hairpin substrate. The longer the capturing time, the more hairpin substrate was disturbed and the stronger background signal was generated. In order to obtain the best signal-to-background ratio, 1 h was chosen as the optimum capturing time.

3.5. Target detection

Fig. 2A exhibited DPV response curves for the relationship between the peak current and the target DNA concentration. The higher the target concentration, the more hairpin substrate became digested and the stronger electrochemical signal was resulted. As shown in Fig. 2A, the peak current increased along with the increasing target DNA concentration ranging from 100 fM to 1 nM. The calibration curve is shown as an inset in Fig. 2B. There was a linear relationship between the target DNA concentration and the peak current in the concentration range from 100 fM to 0.1 nM. The linear regression equation was $y = -43.42x - 0.6209$ (where y is the peak current and x is the target DNA concentration) with a correlation coefficient of 0.9931. As calculated by the 3σ rule (where σ is the standard deviation of the blank signal), a robust detection limit of 50 fM could be achieved. The wide linear range and high sensitivity could be attributed to multiple cleavages of copies of hairpin substrate by the DNAzyme, which gave rise to significantly increased amount of signal probes. Besides, the enzyme amplification reaction also promoted the sensitivity and extends the detection range. This low detection limit was comparable to, or more sensitive than, the detection limits reported previously (Liu et al., 2008; Miranda-Castro et al., 2007; Xiao et al., 2007a,b).

3.6. Selectivity

To evaluate the specificity of the biosensor, eight different DNA sequences (Table 1) including the complementary target DNA, five types of single-base mismatched DNA, the four-base mismatched DNA, and the non-complementary DNA were selected to study the selectivity. Fig. 3A shows the DPV response curves of these eight DNA sequences and the background, and Fig. 3B shows the comparison of the peak currents of these eight DNA sequences

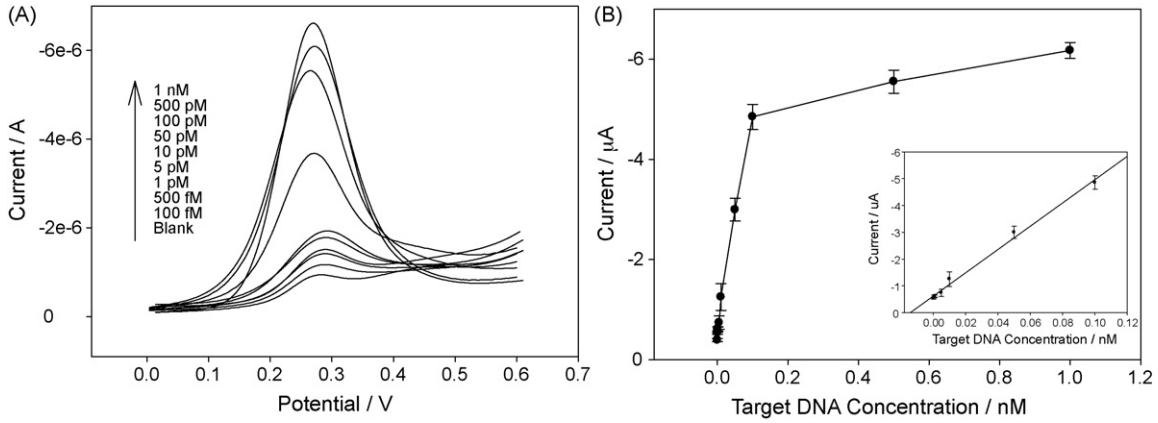

Fig. 2. (A) Differential pulse voltammetry response curves of the biosensor at various target DNA concentrations, from 100 fM to 1 nM. DPV was recorded in a 0.5 M Tris–HCl (pH 9.6) buffer containing 10 mM Mg^{2+} from 0 to 0.6 V under a scan rate of 10 mV/s and a pulse amplitude of 20 mV. (B) The plots of peak currents versus the target DNA concentrations. Error bars are the standard deviation of three repetitive experiments. Inset: linear relationship between the peak current and the target DNA concentrations from 100 fM to 0.1 nM.

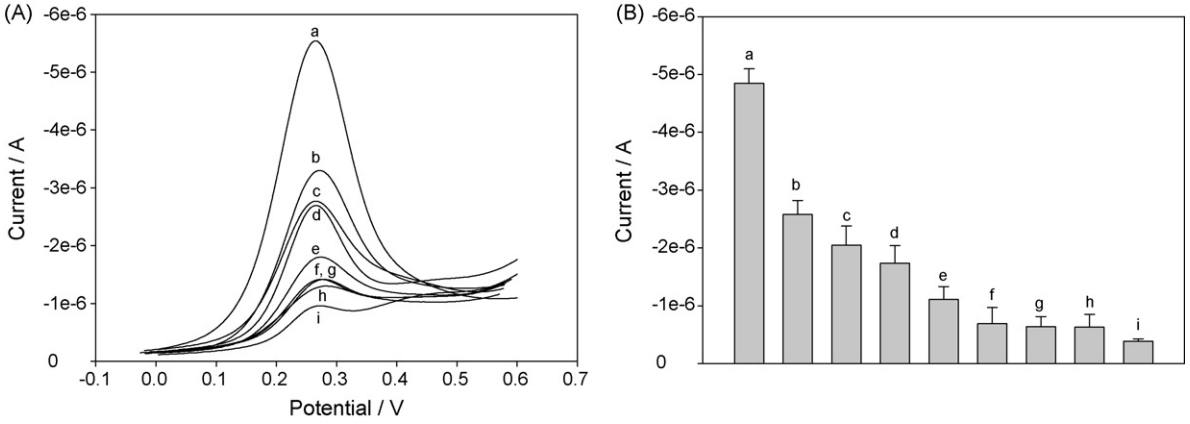

Fig. 3. Specificity investigation. (A) Differential pulse voltammetry response curves at 0.1 nM (a) target DNA, (b) single-base mismatch 4, (c) single-base mismatch 5, (d) single-base mismatch 3, (e) single-base mismatch 2, (f) single-base mismatch 1, (g) four-bases mismatch, (h) non-complementary, and (i) blank. DPV was recorded in a 0.5 M Tris–HCl (pH 9.6) buffer containing 10 mM Mg^{2+} from 0 to 0.6 V under a scan rate of 10 mV/s and a pulse amplitude of 20 mV. (B) Bar chart of the differential pulse voltammetry responses of 0.1 nM (a) target DNA, (b) single-base mismatch 4, (c) single-base mismatch 5, (d) single-base mismatch 3, (e) single-base mismatch 2, (f) single-base mismatch 1, (g) four-bases mismatch, (h) non-complementary, and (i) blank.

and the background. The same amounts (0.1 nM) of seven control sequences and the target DNA were detected after hybridization with the DNAzyme and the hairpin substrate, and the signals of peak currents were recorded. As shown in Fig. 3B, the peak current of the complementary target DNA was −4.849 μA, much higher than those of the control sequences whose peak currents were −0.6957, −1.1090, −1.7370, −2.5800, −2.0460, −0.6392 and −0.6311 μA and the blank background was −0.39 μA. A significant signal difference demonstrated that the biosensor was able to discriminate cDNA as the target with high specificity and sensitivity.

3.7. Regeneration

Regeneration is one of the significant factors of the sensor's performance, which is important for the continuous detection of the target. After the electrochemical detection, the electrode was rinsed with DMF and water to remove any trace of electropolymerized derivative, and finally immersed in hot distilled water at 80 °C for 10 min, followed by a rapid cooling in an ice bath for 10 min. The experimental data (Fig. 4) demonstrated that the shift of peak current response to 0.1 nM target DNA was about 20% after 8 experiments, indicating that the sensor could be easily and successfully regenerated. The signal attenuation might be attributed to the loss

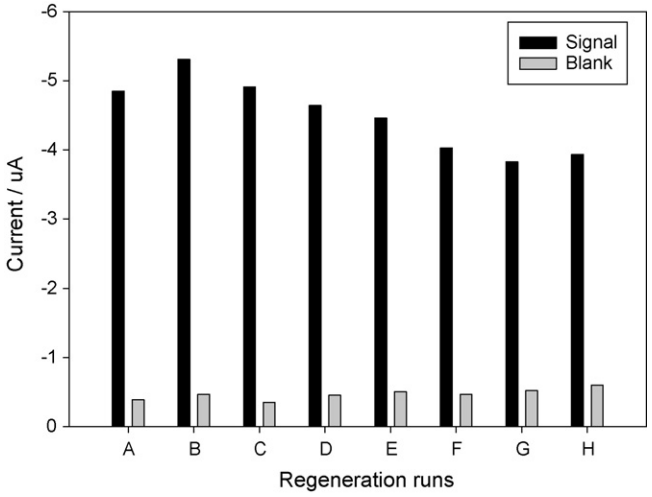

Fig. 4. Typical DPV peak current of the sensor in eight responses and regeneration runs. The concentration of target DNA was 0.1 nM.

of immobilized thiolated capture probes on the gold electrode surface.

4. Conclusion

A new electrochemical DNA biosensor based on proximity-dependent DNA ligation assays with DNAzyme amplification of hairpin substrate signal was constructed for the simple, rapid, specific detection of a short DNA sequence. In the present study, the proximity-dependent ligation assay led to DNA recognition events and the self-organization of DNAzyme structures. The activation of the DNAzyme, in turn, activates multiple cleavages of copies of hairpin substrate and gives rise to significantly increased amount of signal probes. Meanwhile, the biotin–streptavidin interaction has been used for amplifying the signal after hybridization. On the basis of this strategy, the sensor has been applied for detecting complementary target sequences of *H. pylori* over the range from 100 fM to 1 nM with a detection limit of 50 fM. The signal response was also remarkably strong with high reusability. This novel electrochemical DNA biosensor has impressive selectivity with successful discrimination of the target DNA from various mismatched sequences. Therefore, the simple strategy may be of great promise for ultrasensitive DNA detection and be facile to apply in DNA damage analysis and clinical diagnostics.

Acknowledgements

This work was supported by "973" National Basic Research Program of China (No. 2007CB310500) and NSF (20775023, J0830415) of China.

Appendix A. Supplementary data

Supplementary data associated with this article can be found, in the online version, at doi:10.1016/j.bios.2010.04.012.

References

Azek, F., Grossiord, C., Joannes, M., Limoges, B., Brossier, P., 2000. Anal. Biochem. 284, 107–113.
Breaker, R.R., 1999. Nat. Biotechnol. 17, 422–423.
Breaker, R.R., 2000. Science 290, 2095–2096.
Brown, A.K., Li, J., Pavot, C.M.-B., Lu, Y., 2003. Biochemistry 42, 7152–7161.
Cairns, M.J., King, A., Sun, L.-Q., 2000. Nucleic Acids Res. 28, e9.
Carpini, G., Lucarelli, F., Marrazza, G., Mascini, M., 2004. Biosens. Bioelectron. 20, 167–175.
Del Giallo, M.L., Lucarelli, F., Cosulich, E., Pistarino, E., Santamaria, B., Marrazza, G., Mascini, M., 2005. Anal. Chem. 77, 6324–6330.
Elbaz, J., Moshe, M., Shlyahovsky, B., Willner, I., 2009. Chem. Eur. J. 15, 3411–3418.
Fredriksson, S., Gullberg, M., Jarvius, J., Olsson, C., Pietras, K., Gustafsdottir, S.M., Ostman, A., Landegren, U., 2002. Nat. Biotechnol. 20, 473–477.
Gong, H., Zhong, T., Gao, L., Li, X., Bi, L., Kraatz, H., 2009. Anal. Chem. 81, 8639–8643.
Joyce, G.F., 2004. Annu. Rev. Biochem. 73, 791–836.
Lee, J.H., Wang, Z., Liu, J., Lu, Y., 2008. J. Am. Chem. Soc. 130, 14217–14226.
Liu, G., Wan, Y., Gau, V., Zhang, J., Wang, L., Song, S., Fan, C., 2008. J. Am. Chem. Soc. 130, 6820–6825.
Lu, Y., Liu, J., 2006. Curr. Opin. Biotechnol. 17, 580–588.
Lucarelli, F., Marrazza, G., Mascini, M., 2006. Langmuir 22, 4305–4309.
Markham, N.R., Zuker, M., 2005. Nucleic Acids Res. 33, W577–W581.
Miranda-Castro, R., de-los-Santos-Alvarez, P., Lobo-Castanon, M.J., Miranda-Ordieres, A.J., Tunon-Blanco, P., 2007. Anal. Chem. 79, 4050–4055.
Munge, B., Liu, G., Collins, G., Wang, J., 2005. Anal. Chem. 77, 4662–4666.
Osborn, S.E., Ellington, A.D., 1997. Chem. Rev. 97, 349–370.
Sando, S., Sasaki, T., Kanatani, K., Aoyama, Y., 2003. J. Am. Chem. Soc. 125, 15720–15721.
Sando, S., Narita, A., Sasaki, T., Aoyama, Y., 2005. Org. Biomol. Chem. 3, 1002–1007.
Stojanovic, M.N., Prada, P., Landry, D.W., 2001. Chembiochem 2, 411–415.
Takenaka, S., Yamashita, K., Takagi, M., Uto, Y., Kondo, H., 2000. Anal. Chem. 72, 1334–1341.
Tian, Y., Mao, C., 2005. Talanta 67, 532–537.
Tuerk, C., Gold, L., 1990. Science 249, 505–510.
Xiao, Y., Lou, X., Uzawa, T., Plaks, K.I., Plaxco, K.W., Tom Soh, H., 2009. J. Am. Chem. Soc. 131, 15311–15316.
Xiao, Y., Qu, X., Plaxco, K.W., Heeger, A.J., 2007a. J. Am. Chem. Soc. 129, 11896–11897.
Xiao, Y., Rowe, A.A., Plaxco, K.W., 2007b. J. Am. Chem. Soc. 129, 262–263.
Yin, B.-C., Ye, B.-C., Tan, W., Wang, H., Xie, C.-C., 2009. J. Am. Chem. Soc. 131, 14624–14625.
Zhang, X., Li, L., Li, L., Chen, J., Zou, G., Si, Z., Jin, W., 2009a. Anal. Chem. 81, 1826–1832.
Zhang, Y., Huang, Y., Jiang, J.H., Shen, G.L., Yu, R.Q., 2007. J. Am. Chem. Soc. 129, 15448–15449.
Zhang, Y., Wang, Y., Wang, H., Jiang, J.-H., Shen, G.-L., Yu, R.-Q., Li, J., 2009b. Anal. Chem. 81, 1982–1987.